1996 IEEE/SICE/RSJ International Conference on

Multisensor Fusion and Integration for Intelligent Systems

December 8-11, 1996
Washington D.C., U.S.A.

MFI '96

96TH8242

Proceedings of the 1996 IEEE/SICE/RSJ International Conference on Multisensor Fusion and Integration for Intelligent Systems

A New Sensing Scheme for 3D Active Antenna

Naoki Kanayama, Makoto Kaneko *and* Toshio Tsuji

Industrial and Systems Engineering,
Hiroshima University,
Kagamiyama, Higashi-Hiroshima, 739, Japan

Abstract— **This paper discusses a new sensing scheme for 3D Active Antenna that can detect not only the contact location between an insensitive flexible beam and an object but also the normal direction of the object's surface where the beam makes contact. The Active Antenna is simply composed of an insensitive flexible beam, actuators to move the beam, position sensors to measure the rotational angle of the beam, and a moment sensor. In our former work [1], we have shown that both the normal direction and the contact distance can be obtained by more than three times pushing motions. Through the mathematical formulation between the pushing geometry and the contact force, we newly find that both the normal direction and the contact distance can be determined by just one time pushing motion, even though a lateral slip between the beam and an object appears during the pushing motion. We further verify the working principle by experiments.**

Keywords— **Active Antenna, Active Sensing, Contact Distance, Normal Direction, Tactile Sensing**

I. Introduction

Insects have two advanced antennae that can compensate for the limitation of the sensing capability by their vision system. Furthermore, insects seem to use their antennae skillfully so that they may avoid hitting with objects particularly close to them. An interesting observation is that insects are always moving their flexible antennae actively as shown in Fig.1, while crawling, running, and even staying still. The antenna can be characterized by its flexibility and active motions. Active motions might be useful for extending the sensing volume in 3D space, and the flexibility of the antenna would contribute to reducing the impulsive force appeared when the antenna contacts an object unexpectedly. By taking the flexibility and the active motion into considerations, we have proposed a new sensing system, Active Antenna [1], [2], [3], in which both flexibility and active motions essentially contribute to localizing contact point between the antenna and the object.

The Active Antenna is composed of an insensitive flexible beam, actuators to move the beam, position sensors to measure the beam position, and a two (at most)-axis moment sensor to evaluate the contact force. The Active Antenna is a sensing system enabling us to detect the contact location through the measurement of the rotational compliance of an insensitive flexible antenna in contact with an object. While applying a pushing motion for a 3D Active Antenna, a lateral slip may occur according to the direction of pushing, the friction at the point of contact, and the normal surface of the object where the antenna makes contact. Generally, such a lateral slip overestimates the rotational compliance of the antenna which is in contact with the object, and as a result, deteriorates the sensing accuracy directly. Allowing a lateral slip, we have shown a sensing algorithm [1] enabling us eventually to find the direction that avoids any lateral slip based on the sensor information collected during the active motions. Once the normal direction is obtained, the contact distance can be obtained by applying the same way used in 2D model. Because no lateral slip is guaranteed under the pushing motion into the normal direction. However, it requires more than three times pushing motions for guaranteeing the sensing accuracy, and therefore, it is not desirable from the viewpoint of quick sensing.

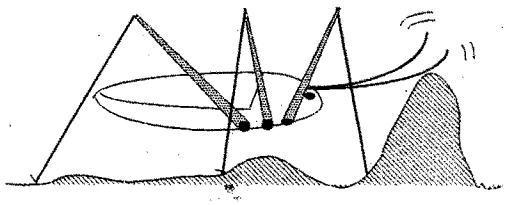

Fig. 1. Insect's antennae.

Through the mathematical formulation between the pushing geometry and the contact force, we newly find that both the normal direction and the contact distance can be obtained by just one time pushing motion, even though a lateral slip appears during the pushing motion. In this paper, we first explain the basic behavior of contact force during both phases of increase and decrease of pushing angle. Then, we formulate the relationship between the pushing angle and the contact force projected on the sensing plane

0-7803-3700-X/96 $5.00

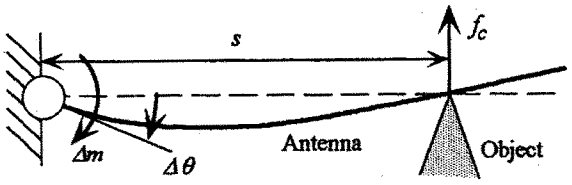

Fig. 2. The 2D Active Antenna.

where the direction of contact force can be detected by two-axis moment sensors. Although the relationship includes the normal direction of the object's surface as an unknown parameter, we show that the normal direction can be determined by the geometrical relationship obtained from each of the increase and the decrease of pushing angle.

After reviewing conventional works in chapter II, we briefly explain the basic working principle of 2D and 3D Active Antenna in chapter III. The basic behavior of contact force is precisely discussed in chapter IV. Then, the one pushing motion sensing strategy is proposed in chapter V. In chapter VI, we show a couple of experimental results to verify the proposed sensing scheme. Finally, we conclude our work in chapter VII.

II. Conventional Works

There have been a number of works discussing insect's antennae-like sensor or whisker type sensor. For example, a simple flexible beam sensor can take the form of a short length of spring piano wire or hypodermic tubing anchored at the end. When the free end touches an external object, the wire bends. This can be sensed by a piezoelectric element or by a simple switch [4]. A more elaborate sensor is described by Wang and Will [5]. Long antennae-like whisker sensors were mounted on the SRI mobile robot, Shakey [6], and on Rodney Brook's six-legged robot insects [7]. Hirose, et. al. discussed the utilization of whisker sensors in legged robots [8]. The sensor system is composed of an electrode and a whisker whose end is fixed at the base. This sensor unit has been arranged in an array around each foot of the legged robot, Titan III, so that it can monitor the separation between each foot and the ground to allow deceleration of the foot before contact. Similarly shaped whsensingiskers have been considered for legs of Ohio State University active suspension vehicle [9]. Russell has developed a sensor array [10] by mounting whisker sensors on a mobile robot, and succeeded in reconstructhe shape of a convex object followed by the whiskerWilson and Mahajan [11], Snyder and Wilson [12] have designed the whisker probe system composed of a piano wire with strain gage sensors and the base sweep actuators made of two polyurethane tubes that bend when pressurized with air. Wilson and Chen [13] have reported experimental results that demonstrate the precision and accuracy of the whisker probe system in detecting andisplaying solid boundaries enclosing areas up to 40 cm by 50 cm. These works also assume that the whisker tip always makes contact with the object. The major difference between previous works [4]-[13] and ours is that the Active Antenna can localize a contact point between the insensitive oughantenna and the object, while previous works do not.

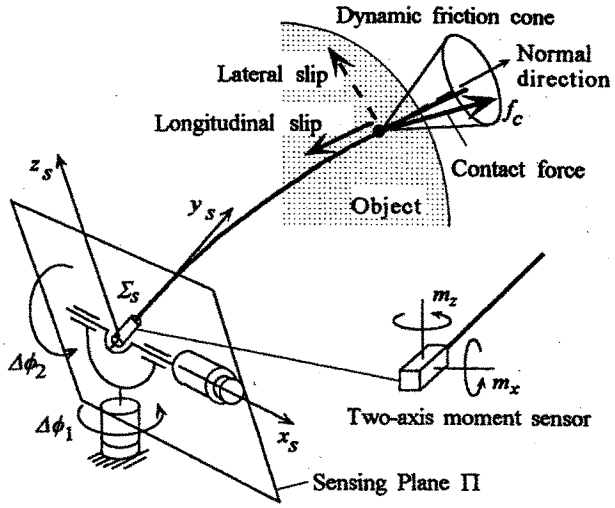

Fig. 3. Basic structure of the 3D Active Antenna.

III. 2D and 3D Active Antenna

A. Assumptions

Assumption 1: The object is rigid.

Assumption 2: The object is stationary during active motions.

Assumption 3: The deformation of the beam is small enough to ensure that we can apply linear approximation.

Assumption 4: The elongation of the beam due to a unit axial force is negligibly small compared with the deflection due to a unit bending force.

Assumption 5: The beam has a uniform compliance in a plane perpendicular to the longitudinal axis.

Assumption 6: The object has an extremely small curvature along the axial direction of the beam and a large curvature perpendicular to the axial direction.

Assumption 7: Dynamic effects are neglected.

Assumptions 1 and 2 mean that the measured moment is caused only the pushing motion of the antenna. Assumption 3 can be conveniently utilized for extracting a simple result from a set of nonlinear equations. Assumption 4 implies that the antenna is extremely stiff in its axial direction, while it is relatively much complaint in non-axial direction. A uniform beam having a circular cross section, such as a piano wire can satisfy assumption 5. For such a beam, the direction of reaction force is exactly collinear with that of the beam deflection, which can be conveniently utilized for judging the occurrence of the lateral slip. With assumption 6, we neglect the effect of the object's curvature on the sensing accuracy for simplifying the discussion.

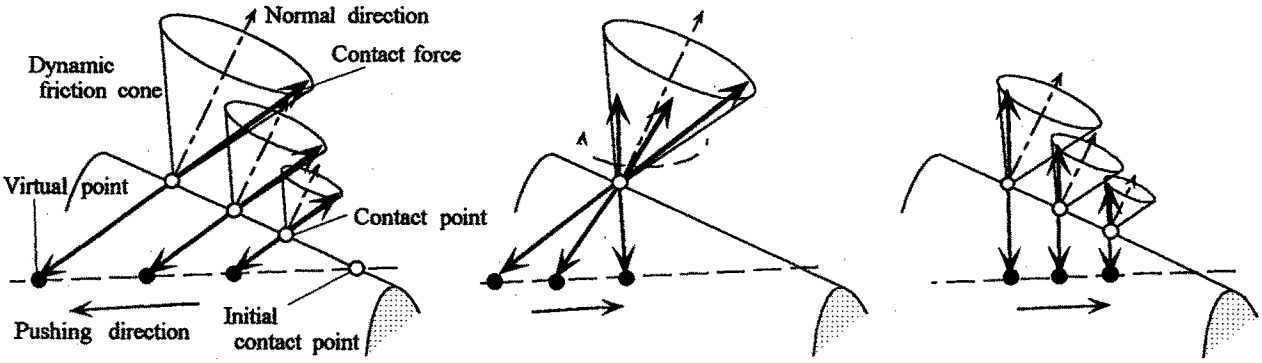

(a) Phase A : Pushing phase (b) Phase B : Turning phase (c) Phase C : Returning phase

Fig. 4. Basic behaviors of contact force during sensing motion.

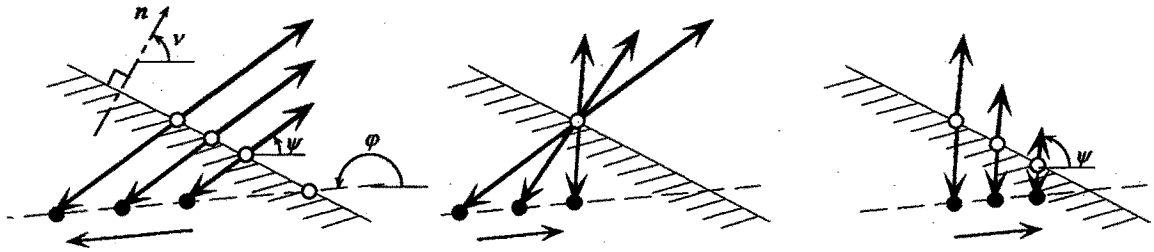

(a) Phase A : Pushing phase (b) Phase B : Turning phase (c) Phase C : Returning phase

Fig. 5. Basic behaviors of contact force projected on sensing plane Π.

B. Working principle of 2D and 3D Active Antenna

Now, let us briefly explain the basic working principle of 2D and 3D Active Antenna. For the 2D Active Antenna [2] as shown in Fig.2, it can detect the distance through the measured compliance of the antenna in contact with an object. Basic relationship between deformation of the beam and contact force for 2D model is given by

$$\Delta r = \frac{\Delta f}{k} s^3, \tag{1}$$

where Δf and Δr denote the contact force of the beam and the deformation length under a contact force. If there is no object, the beam has the following displacement at the point of the contact.

$$\Delta r \approx s\Delta\theta, \tag{2}$$

where the rotation angle $\Delta\theta$ is sufficiently small to satisfy assumption 3. Also there is the following relation

$$\Delta m = s\Delta f, \tag{3}$$

where Δm denotes the moment measured on the center of rotation. From eqs.(1), (2) and (3), we can get the contact distance s expressed by eq.(4).

$$s = kC_\theta \tag{4}$$

where C_θ is the rotational compliance of the beam in contact with an object and k is a constant concerned with the stiffness of the beam. Since $C_\theta = \Delta\theta/\Delta m$, we can estimate a contact distance by utilizing both moment and position sensor outputs. For 2D model, we implicitly assume that there is no lateral slip during a pushing motion. Once a lateral slip occurs, 2D model no more works appropriately. To cope with a lateral slip, we have designed and developed the 3D Active Antenna.

Figure 3 shows an overview of the 3D Active Antenna and its coordinate system, where Σ_s denotes the sensor coordinate system. The 3D Active Antenna is composed of an insensitive flexible beam, two actuators to move the beam in 3D space, two position sensors to measure the angular displacements ϕ_1 and ϕ_2, and a two-axis moment sensor to detect moments around both x_s and z_s axes. Now, let us define the sensing plane Π, as the plane spanned by two unit vectors whose directions coincide with x_s and z_s. The design orientation taken for the two-axis moment sensor enables us to evaluate the direction of the contact force projected on the plane Π from the outputs of the moment sensor. Although we can not measure the contact force directly, we can estimate the direction of contact force projected on the sensing plane Π by utilizing the output from the two-axis moment sensor. From $m_x = sf_z$ and $m_z = sf_x$, we can obtain the direction of the contact force ψ as

$$\psi = \tan^{-1}(f_z/f_x) = \tan^{-1}(m_x/m_z). \tag{5}$$

Therefore, m_x/m_z shows the direction of contact force projected on the sensing plane Π. For the 3D Active Antenna, the pushing and the contact force directions are regarded as input and output, respectively. For an arbitrary push-

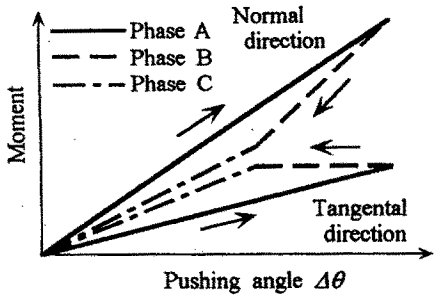

(a) Moment sensor output.

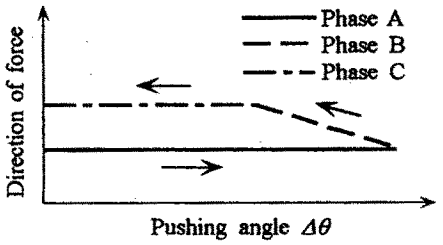

(b) Estimated direction of contact force.

Fig. 6. An example of moment and direction of the force in sensing motion.

ing, the beam makes slip not only the longitudinal direction but also the lateral direction as shown in Fig.3. By using the input-output relationship, the 3D Active Antenna can finally reach the normal direction of the object's surface after a number of trials. Once the normal direction is detected, the contact distance can be evaluated by applying the same way taken in 2D model. These are the outline of our former works. However, in our former approach [1] requires many trials to find the normal direction, as a result, it needs non-negligible sensing time.

IV. Basic Behavior of Contact Force

A. Basic behavior of contact force in 3D space

During a pushing motion, the contact point always makes slip on the object's surface where the beam makes contact. Now, let us consider the basic behavior of contact force during pushing and returning phases. We consider a pushing and a returning motions as a set of sensing motion in this work. We can roughly classify the behavior of the contact force into three phases as shown in Fig.4.

Phase A: Pushing phase

Figure 4(a) shows the relationship between the pushing distance and the contact force during pushing phase, where each black circle denotes the virtual point meaning that the beam passes along the dotted line involving black circles under the absence of object. Actually, however, the beam is blocked by the object and can not move along the dotted line. As a result, the beam deforms according to the surface geometry of object. Each white circle denotes the actual contact point between the beam and the object. Note that the direction of the contact force is always collinear with the line segment between the virtual and the contact points. Because the actual displacement of the

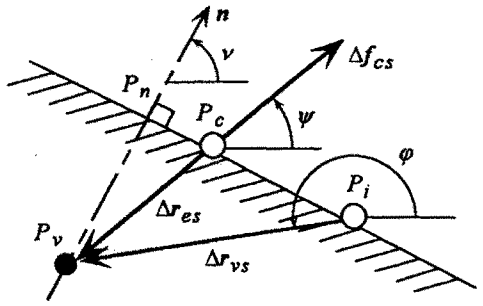

Fig. 7. Notations on the sensing plane Π (Phase A).

beam is given by the distance between the white and the black circles, and the contact force always appears in the opposite direction of the displacement vector. Also note that the magnitude of the contact force is proportional to the pushing distance.

Phase B: Turning phase

When a pushing motion is over, each actuator is commanded so that the virtual point may move toward the initial contact point. At a short time after switching, the contact force changes its direction according to the virtual point as shown in Fig.4(b). We call the particular phase turning phase. Of course, the turning phase will disappear under frictionless contact. Note that during this phase, the lateral shift of the contact point is negligible, while the longitudinal slip appears.

Phase C: Returning phase

After the turning phase, the contact force starts to linearly decrease according to the movement of the virtual point as shown in Fig.4(c). We call this phase returning phase. An important feature is that the magnitude of the contact force is proportional to the pushing distance between the initial contact and each virtual points.

B. Basic behavior of contact force for sensing plane Π

Figure 5 shows several physical parameters projected on the sensing plane Π, where ν, ψ and φ denote the normal direction of the object's surface, the direction of the contact force, and the pushing direction with respect to Σ_s, respectively. Note that ψ and φ are known, while ν is unknown. In either pushing or returning phase, the direction of the contact force ψ does not change for the object having a constant slope during the shift of the virtual point while its magnitude proportionally varies according to the position of the virtual point.

Figure 6 shows a basic behavior of the output from the two-axis moment sensor and the estimated direction of the contact force during a sensing motion. As seen in Fig.6(a), there are two lines with hysteresis characteristics, one is the normal component for the pushing direction and the other is the tangential component. From this moment information, we can estimate the direction of the contact force using eq.(5) as shown in Fig.6(b).

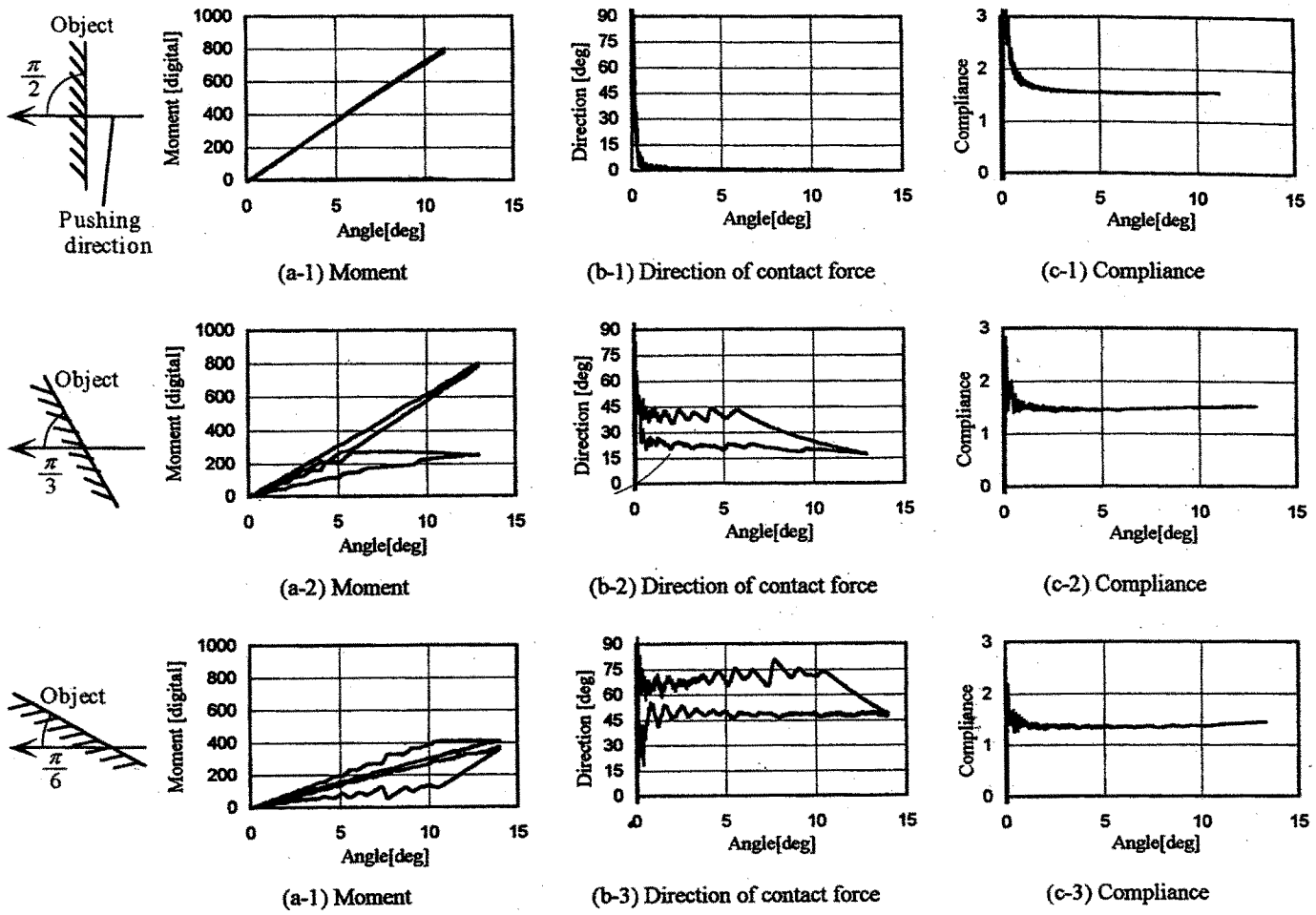

Fig. 8. Experimental results for various pushing directions.

V. One-Pushing-Motion Sensing Scheme

For the 2D Active Antenna, we have the following relation from eqs.(2) and (3)

$$C_\theta = \frac{1}{s^2}\frac{\Delta r}{\Delta f}. \tag{6}$$

For the 3D Active Antenna, we have the similar relationship given by

$$C_\theta = \frac{1}{s^2}\frac{\|\Delta \boldsymbol{r}_{es}\|}{\|\Delta \boldsymbol{f}_{cs}\|}, \tag{7}$$

where $\Delta \boldsymbol{r}_{es}$ and $\Delta \boldsymbol{f}_{cs}$ denote the effective deformation vector and the contact force projected on the sensing plane II. $\|\Delta \boldsymbol{f}_{cs}\|$ is given by $\|\Delta \boldsymbol{f}_{cs}\| = \|\Delta \boldsymbol{m}\|/s$ where $\|\Delta \boldsymbol{m}\| = \sqrt{\Delta m_x^2 + \Delta m_z^2}$. The effective deformation vector cannot measure directly, but the relationship between $\|\Delta \boldsymbol{r}_{es}\|$ and $\|\Delta \boldsymbol{r}_{vs}\|$ can be formulated easily. Figure 7 shows the vector relationship during a sensing motion in phase A, where P_i, P_v, P_c and P_n denote the initial contact point, the virtual point, the actual contact point and the intersection between the perpendicular line from P_v and the object surface, respectively. The line segment P_vP_n is common for two triangles $P_iP_vP_n$ and $P_cP_vP_n$. Taking this relationship into consideration, we can obtain the relationship between $\|\Delta \boldsymbol{r}_{es}\|$ and $\|\Delta \boldsymbol{r}_{vs}\|$ in the following, using parameters in Fig.7

$$\|\Delta \boldsymbol{r}_{es}\|\cos(\nu - \psi) = \|\Delta \boldsymbol{r}_{vs}\|\cos(\nu - \varphi). \tag{8}$$

By using eq.(8), eq.(7) can be rewritten as follows

$$C_\theta = \frac{1}{s^2}\frac{\|\Delta \boldsymbol{r}_{vs}\|}{\|\Delta \boldsymbol{f}_{cs}\|}\frac{\cos(\nu - \varphi)}{\cos(\nu - \psi)}. \tag{9}$$

Taking $\|\Delta \boldsymbol{r}_{vs}\| = s\Delta\theta$ into consideration, eq.(9) can be further rewritten by

$$C_\theta = \frac{\Delta\theta}{\|\boldsymbol{m}\|}\frac{\cos(\nu - \varphi)}{\cos(\nu - \psi)}. \tag{10}$$

Equation (10) has two unknown variables C_θ and ν. It is obvious from Fig.5(a) and (c) that $\Delta\theta/\|\boldsymbol{m}\|$ and φ are constant during both the pushing and the returning phases, while ψ varie according to either the pushing or the returning phase. Now let us choose one from each of pushing and returning phase.

$$C_\theta = \frac{\Delta\theta_1}{\|\boldsymbol{m}_1\|}\frac{\cos(\nu - \varphi)}{\cos(\nu - \psi_1)} \tag{11}$$

$$C_\theta = \frac{\Delta\theta_2}{\|\boldsymbol{m}_2\|}\frac{\cos(\nu - \varphi)}{\cos(\nu - \psi_2)} \tag{12}$$

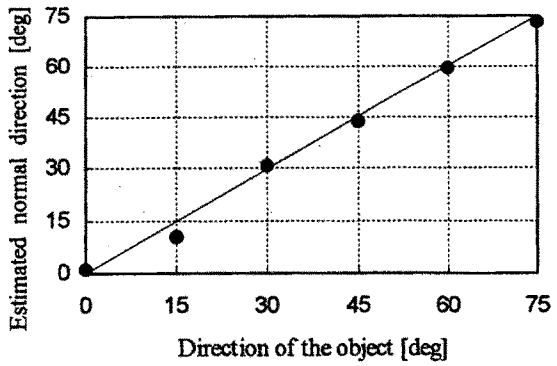

Fig. 9. Estimated direction of the contact force.

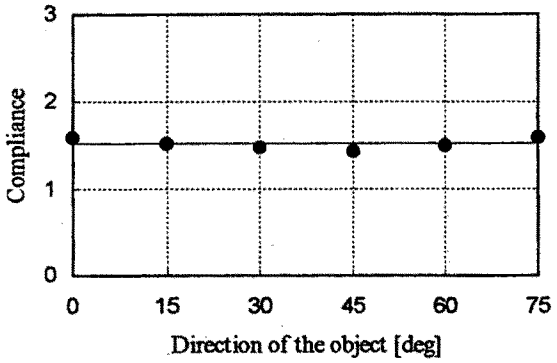

Fig. 10. Estimated compliance.

where the subscript "1" and "2" denote the pushing and the returning phase, respectively. From eqs.(11) and (12), we can get the following equation,

$$\frac{\Delta\theta_1}{\|\boldsymbol{m}_1\|}\frac{1}{\cos(\nu-\psi_1)} = \frac{\Delta\theta_2}{\|\boldsymbol{m}_2\|}\frac{1}{\cos(\nu-\psi_2)}. \qquad (18)$$

Since eq.(13) can be regarded as an equation for unknown variable ν, ν can be determined by solving this equation. If we can assume $\Delta\theta_1/\|\boldsymbol{m}_1\| = \Delta\theta_2/\|\boldsymbol{m}_2\|$ as a possible case, then we can find the following solution

$$\nu = \frac{\psi_1+\psi_2}{2}. \qquad (14)$$

Equation (14) means that the normal direction of the object is an arithmetic mean of two measured directions of the contact force. Once ν is determined by solving eq.(13), C_θ can be computed by utilizing either eq.(11) or eq.(12). Therefore, the relationship between C_θ and s becomes known. These discussions prove that one set of the pushing and the returning motion is sufficient for determining the contact distance as well as the normal direction of the object.

VI. Experiments

Figure 8 shows several experimental results for various directions under the same contact distance, where (a-i), (b-i) and (c-i) ($i = 1,2,3$) are the measured moment, the estimated direction of the contact force, and the compliance, respectively. When the pushing motion is applied for the normal direction to the object, the z-axis output of the moment sensor increases proportionally according to the pushing angle, while the x-axis output keeps zero. When the pushing motion is applied for the direction except the normal one, both x and z-axis outputs appear with the hysteresis characteristics, which is caused by the friction at the point of the contact. As shown in Fig.8(c-i), the computed compliance keeps almost constant except particularly small pushing angle. Figure 9 and 10 show the estimated normal direction of the object and the compliance with respect to the pushing angle, where the all experiments are executed under the same contact distance. It can be seen from Fig.9 that the estimation of the normal direction is fairly good. It is observed from Fig.10 that every computed compliance becomes almost same irrespective of the pushing direction. These results support the validity of the proposed one-pushing-motion sensing scheme.

VII. Conclusion

We proposed a new sensing scheme for the 3D Active Antenna. The proposed scheme ensures to detect not only the contact distance between an insensitive flexible beam and an object but also the normal direction of the object through one pushing motion only. The basic equations were derived and the experimental results were also shown to verify the idea proposed in the paper.

Finally, the authors would like to express their sincere gratitude to Mr. Jiro Chiba, Harmonic Drive Systems Co.Ltd. for his warm support of this work.

References

[1] Kaneko, M., N. Kanayama, T. Tsuji : 3-D Active Antenna for Contact Sensing, *Proc. of the 1995 IEEE Int. Conf. on Robotics and Automation*, pp1113–1119, 1995.

[2] Kaneko, M: Active Antenna, *Proc. of the 1994 IEEE Int. Conf. on Robotics and Automation*, pp2665–2671, 1994.

[3] Kaneko, M., N. Ueno, and T. Tsuji, Active Antenna (Basic Working Principle), *Proc. of the 1994 IEEE Int. Conf. on Intelligent Robotics and Systems*, pp1744–1750, 1994.

[4] Russell, R. A.: Closing the sensor-computer-robot control loop, *Robotics Age*, April, pp15–20, 1984.

[5] Wang, S. S. M., P. M. Will: Sensors for computer controlled mechanical assembly, *The Industrial Robot*, March, pp9–18, 1978.

[6] McKerrow, P.: Introduction to Robotics, *Addison-Wesley*, 1990.

[7] Brooks, R. A.: A robot that walks; Emergent behaviors from a carefully evolved network, *Neural Computation*, vol.1, pp253–262, 1989.

[8] Hirose, S., et. al.: Titan III: A quadrupled walking vehicle, *Proc. of the Second Int. Symp. on Robotics Research*, MIT Press, Cambridge, Massachusetts, 1985.

[9] Schiebel, E. N., H. R. Busby, K. J. Waldron: Design of a mechanical proximity sensor, *Robotica*, vol.4, pp221–227, 1986.

[10] Russell, R. A. : Using tactile whiskers to measure surface contours, *Proc. of the 1992 IEEE Int. Conf. on Robotics and Automation*, pp1295–1300, 1992.

[11] Wilson, J. F., and U. Mahajan: The mechanics and positioning of highly flexible manipulator limbs, *ASME J. of Mechanisms, Transmissions and Automation in Design*, vol.111, pp230–237, 1989.

[12] Snyder, J. M., and J. F. Wilson: Dynamic of the elastica with end mass and follower loading, *ASME J. of Applied Mechanics*, vol.57, pp203–208, 1990.

[13] Wilson, J. F., and A. Chen: A whisker probe system for shape perception of solids, *ASME J. of Dynamic Systems*, Measurement, and Control, vol.117, pp104–108, 1995.

1996 IEEE/SICE/RSJ International Conference on Multisensor Fusions and Integration for Intelligent Systems

IEEE Catalog Number 96TH8242

ISBN 0-7803-3700-X (softbound)
0-7803-3701-8 (microfiche)

Library of Congress 96-78658

Additional copies of this publication are available from

IEEE Operations Center
P.O. Box 1331
445 Hoes Lane
Piscataway, NJ 08855-1331 USA

1-800-678-IEEE
1-908-981-1393
1-908-981-9667 (FAX)
833-233 (Telex)
email: customer.services@ieee.org